Microporous and Mesoporous Materials 190 (2014) 54–62

Contents lists available at ScienceDirect

Microporous and Mesoporous Materials

journal homepage: www.elsevier.com/locate/micromeso

Short Communication

An acid-free route for the facile synthesis of iron-functionalized mesoporous silicas: Transformation between hollow nanospheres and cage-like mesostructures

Hongchuan Xin [a,b], Jiao Zhao [a], Xiaobo Li [a], Jianting Tang [a], Qihua Yang [a,*]

[a] State Key Laboratory of Catalysis, Dalian Institute of Chemical Physics, Chinese Academy of Sciences, 457 Zhongshan Road, Dalian 116023, China
[b] Key Laboratory of Biofuels, Qingdao Institute of Bioenergy and Bioprocess Technology, Chinese Academy of Sciences, 189 Songling Road, Qingdao 266101, China

ARTICLE INFO

Article history:
Received 1 October 2013
Received in revised form 7 January 2014
Accepted 14 January 2014
Available online 27 January 2014

Keywords:
Acid-free
Iron
Mesoporous
Hollow nanospheres
FDU-12

ABSTRACT

Iron-substituted silicas with hollow nanospherical morphology and cage-like mesostructure have been synthesized using triblock copolymer F127 as surfactant and tetramethoxysilane (TMOS) as silica source with no necessary addition of mineral acids. Iron-functionalized hollow nanospheres were obtained using $Fe(acac)_3$ as iron source. When $Fe(NO_3)_3$ was employed as iron source, iron-containing cage-like FDU-12 mesostructure and hollow nanospheres were formed with Fe/Si molar ratio lower than 0.008 and higher than 0.015, respectively. The formation of hollow spheres at high Fe/Si ratio can be regarded as gradually dissociation of nanocages from Fe-FDU-12. The structure of the iron centers was determined by spectroscopic methods (UV–vis and UV–Raman measurements) and by elemental analyses. The facile structural evolution between cage-like and nanospherical structures may be helpful for further understanding the formation mechanism of mesoporous silicas.

1. Introduction

Mesoporous silicas have attracted much attention in last decades due to their wide applications in adsorption, catalysis, and drug delivery [1–4]. Metal-containing mesoporous silicas are of great interest because these functionalized silicas are extremely attractive as catalysts for acid–base, redox, and alkylation reactions [5–7]. One-pot hydrothermal synthesis is preferred for the preparation of metal-substituted mesoporous silicas in the presence of structure-directing agents under acidic [8], neutral [9], or basic [10] conditions.

For transition-metal substituted mesoporous silicas, it is apparent that the transition metal center and the porous structure both play important roles in obtaining desirable properties. Attributed to the development in the material science, the silicas with different morphology and mesostructure have been successfully synthesized [11,12]. However, only limited attention has been paid to the structure and morphology control of the transition-metal substituted mesoporous silicas, partly due to the unmatched conditions for the incorporation of transition metal ions and the formation of silicas with controlled morphology and mesostructure. For example, the nonionic-surfactants (such as P123, F127) have been widely used as templates for the fabrication of mesostructured silicas normally in strongly acidic conditions [13]. However, the highly acidic media are not ideal for incorporation of transition-metal ions due to the high solubility of the Si–O–M species. The previous studies show that the mild reaction media may solve this problem [14–17], but the structural and morphological control of silicas in mild reaction medium is not well developed yet.

It is still a challenge to synthesize transition-metal functionalized mesoporous silicas with desirable active metal centers (such as highly isolated metal sites [18]) and architectures (such as spherical and cage-like pore structures). Among the silica fibers, spheres, rods and nanoparticles, the hollow nanospheres are very attractive, given that the hollow interior can encapsulate the guest molecules for wide application potentials [19–28]. The modification of the shell of the hollow nanospheres may further expand the application potentials of the hollow nanospheres [29–35]. The strategies for the synthesis of hollow silica-based nanospheres were already well reviewed [36,37], and can be categorized as: selective etching or dissolution, soft templating, self templating, galvanic replacement method, and Ostwald ripening method, etc. Based on the composition and structure, the obtained hollow nanospheres can be classified as pure siliceous nanospheres [38,39], phosphosilicate nanospheres [40], multi-shell silica nanospheres [32,41], organo-functionalized silica nanospheres [22,42], and yolk-shell nanoparticles [34,37], etc. Our group has developed an

* Corresponding author. Tel.: +86 411 84379552; fax: +86 411 84694447.
E-mail address: yangqh@dicp.ac.cn (Q. Yang).

http://dx.doi.org/10.1016/j.micromeso.2014.01.019
1387-1811/

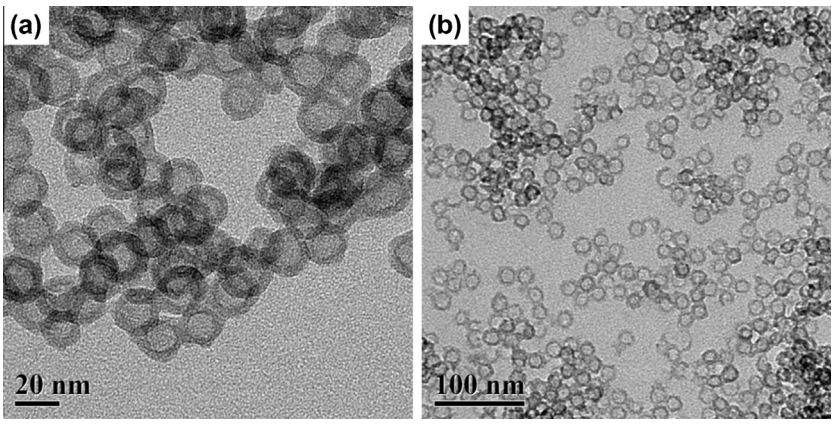

Fig. 1. TEM images of Fe-substituted hollow nanospheres: (a) NS-0.8 and (b) NS-1.5.

easy, convenient and efficient method for the green synthesis of hollow nanospheres in deionized water without any mineral acid addition [43]. The neutral synthesis medium may provide an opportunity for the effective incorporation of transition-metal ions in the shell of the hollow nanospheres.

To the best of our knowledge, the synthesis of transition metal ion-substituted hollow nanospheres *via* direct hydrothermal route has rarely been reported. In this study, based on our previous study [43], we report the facile synthesis of Fe-containing silica hollow nanospheres in acid-free neutral medium using F127 as the structure-directing agent. In addition, the evolution of hollow nanosphere to cage-like FDU-12 mesostructure was observed by simply varying the iron precursor and Fe/Si molar ratio.

2. Experimental sections

2.1. Reagents

All materials were of analytical grade and used as received without any further purification. Pluronic F127 ($EO_{106}PO_{70}EO_{106}$) was purchased from Sigma–Aldrich Company Ltd. (USA). Tetramethoxysilane (TMOS), 1,3,5-trimethylbenzene (TMB), $Fe(NO_3)_3{\cdot}9H_2O$, $Fe(acac)_3$, and K_2SO_4 were obtained from Shanghai Chemical Reagent, Inc. of Chinese Medicine Group.

2.2. Synthesis

For the synthesis of Fe-substituted hollow nanospheres, F127 (1.00 g), TMB (1.00 g), and K_2SO_4 (3.49 g) were dissolved in water (60 mL), and the solution was stirred at 13.5 °C for 2 h. Desired amount of $Fe(acac)_3$ dissolved in TMOS (3.04 g) was added to the above surfactant solution. After stirring at 13.5 °C for 24 h, the mixture was transferred into a Teflon-lined autoclave and aged at 100 °C for another 24 h. The precipitate was filtered off, rinsed repeatedly with water and dried at 100 °C. The as-synthesized sample was calcined in air at 550 °C for 10 h with a ramp of 1 °C min^{-1}. The calcined samples were denoted as NS-*n* (*n* = 0.8 or 1.5), where *n* is the mol% of Fe/Si in the initial mixture.

NO_3-NS-*n* (*n* = 0.8, 1.5, and 2.3) samples were synthesized using a method similar to NS-*n* samples with slight variation. $Fe(NO_3)_3$ was used as iron source and the molar ratio of H_2O/F127 is 28000 (the H_2O/F127 molar ratio for NS-*n* is 42000). The calcined samples were denoted as NO_3-NS-*n* (*n* = 0.8, 1.5, and 2.3), where *n* is the mol% of Fe/Si in the initial mixture.

In order to investigate the role of TMB in the synthesis process, NS*-0.8 and NO_3-NS*-0.8 were synthesized with the same procedures to NS-0.8 and NO_3-NS-0.8, respectively, except for the addition of TMB.

2.3. Characterization

X-ray diffraction (XRD) patterns were recorded on a Rigaku RINT D/Max-2500 powder diffraction system using Cu Kα radiation of 0.15406 nm wavelength. The nitrogen sorption experiments were performed at −196 °C on a Micromeritics ASAP 2020 system. Prior to the measurement, the materials were out-gassed at 120 °C for at least 6 h. The Brunauer–Emmett–Teller (BET) specific surface areas were calculated using the adsorption data in the relative pressure (P/P_0) range of 0.05–0.25. Pore size distributions were calculated using the Barrett–Joyner–Halenda (BJH) method based on the adsorption branch and Horvath–Kawazoe (HK) method. The total pore volumes were estimated from the amount adsorbed at a relative pressure P/P_0 of 0.99. Transmission electron microscopy (TEM) was performed using a JEOL JEM-2000EX and a FEI Tecnai G^2 Spirit at an acceleration voltage of 120 kV. Field-emission scanning electron microscopy (FESEM) was undertaken on a HITACHI S-4800 microscope operating at an accelerating voltage of 1–30 kV. UV–vis diffuse reflectance spectra were recorded on a JASCO V-550 UV–vis spectrophotometer. The powder material was loaded into a quartz cell, and the spectra were collected in the range of 190–800 nm with $BaSO_4$ as the reference. UV resonance Raman spectra were measured at room temperature with a Jobin-Yvon T64000 triple-stage spectrograph with a spectral resolution of 2 cm^{-1} [44]. The 290 nm line from a Coherent Innova 300 Fred laser was used as an excitation source. The power of the 290 nm line at samples was below 1.0 mW. The Si content of the samples was determined by X-ray fluorescence spectrometer (XRF, Axios PW4400, Panalytical), and the Fe content was measured with Inductively Coupled Plasma Optical Emission Spectrometry (ICP-OES, IRIS Intrepid II XSP, Thermo Fisher) after the sample was dissolved in a mixture of HF and HNO_3. The ammonia temperature-programmed desorption (NH_3-TPD) was measured on a Micromeritics Autochem 2920 instrument. The catalyst (0.15 g) was charged in a U-shaped quartz cell and pretreated in Ar (20 mL min^{-1}) at 500 °C for 1 h (ramp rate 10 °C min^{-1}), then cooled down to 100 °C followed by changing the gas flow to a mixture of 10% NH_3-90% Ar (40 mL min^{-1}) for 2 h. The sample was then purged with Ar (20 mL min^{-1}) at 100 °C for 2 h to remove free and weakly adsorbed ammonia. The NH_3-TPD profile was obtained by rising the temperature up to 550 °C (ramp rate 10 °C min^{-1}), using a TCD detector.